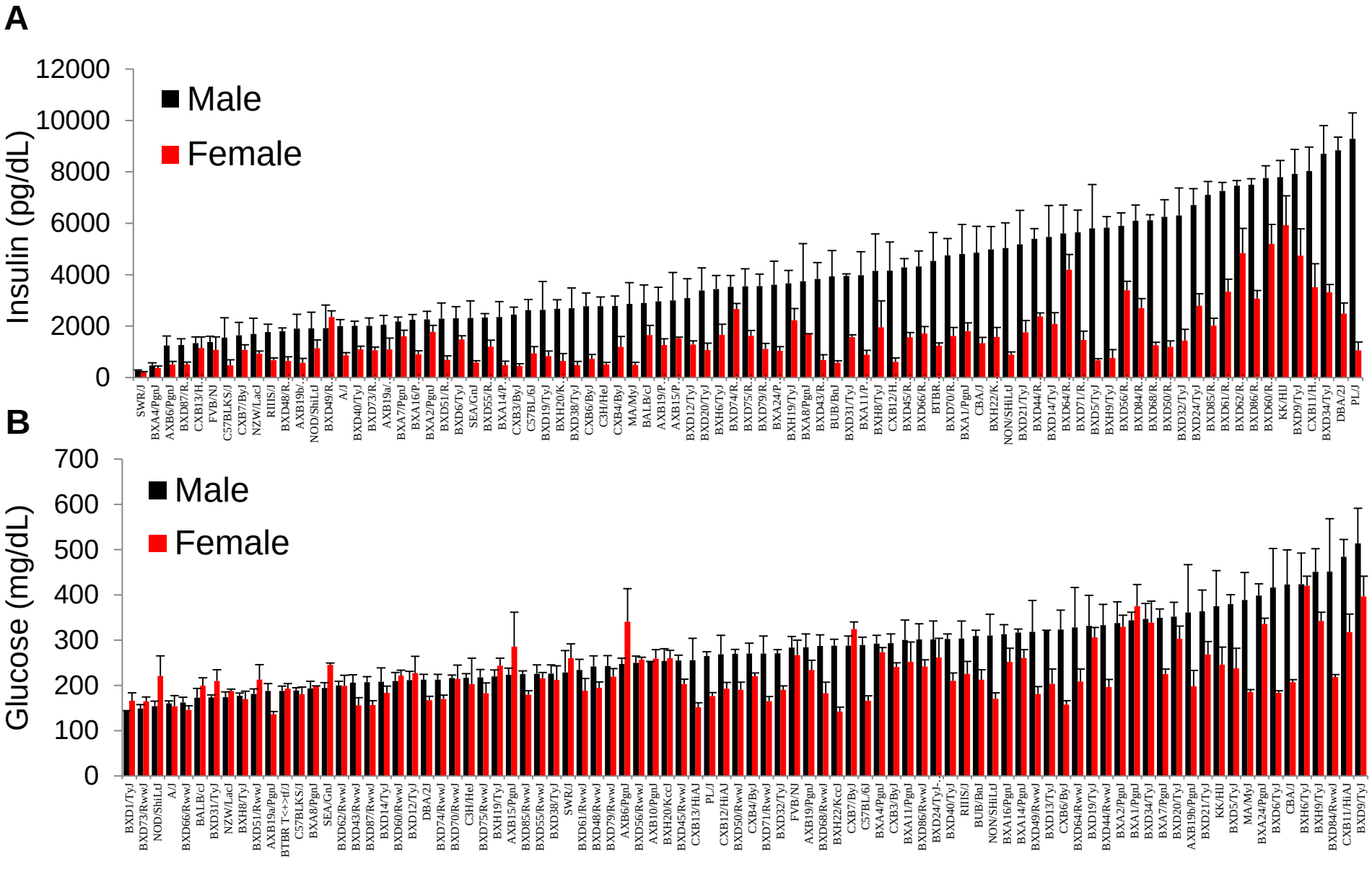

Figure S1. Variation in plasma insulin and glucose among male and female strains, Related to Figure 1

(A) Plasma insulin levels in male (black) and female (red) mice after 8 weeks of HF/HS feeding. Error bars represent SEM.

(B) Plasma glucose levels in male (black) and female (red) mice after 8 weeks of HF/HS feeding. Error bars represent SEM.

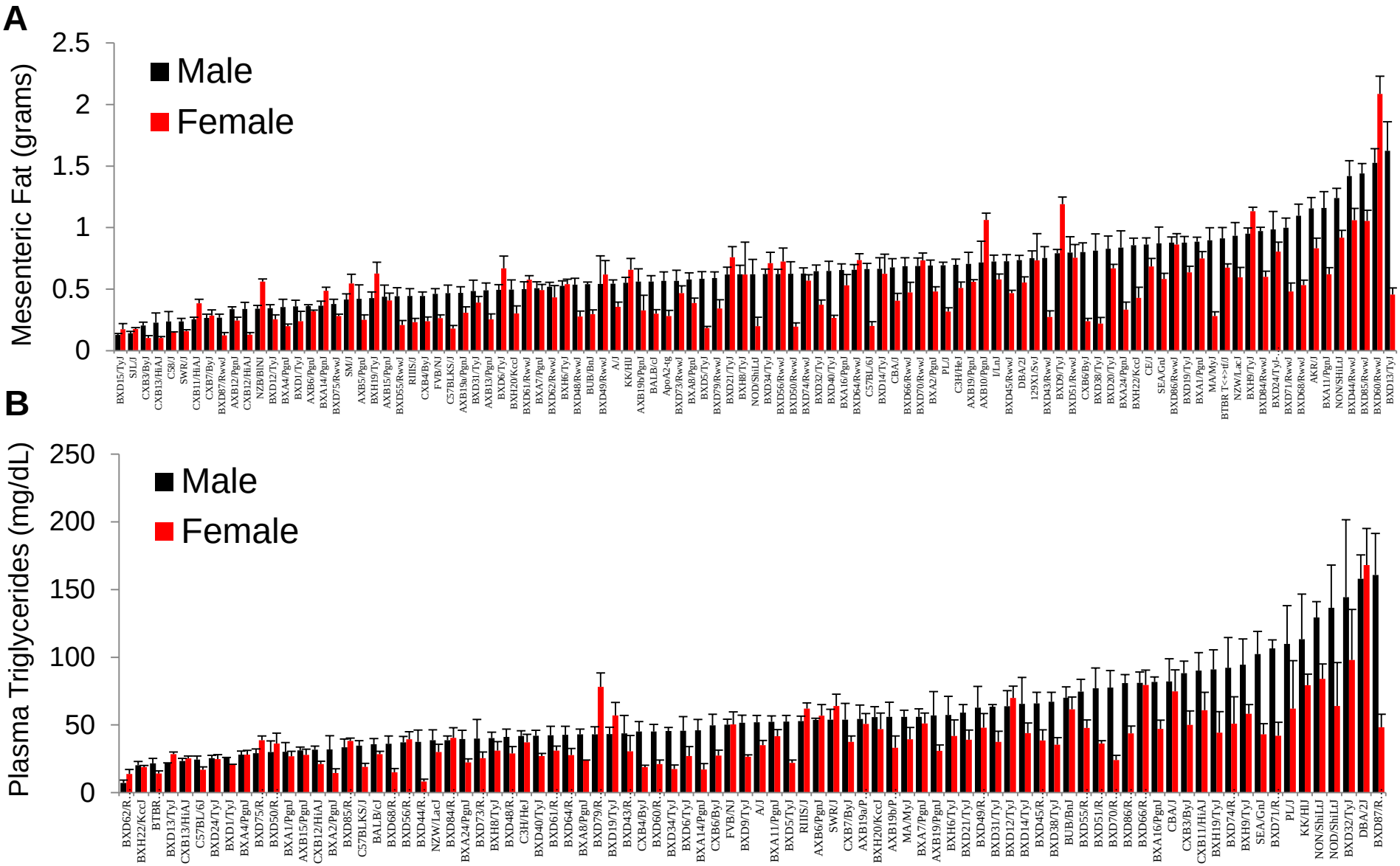

Figure S2. Variation in central obesity and plasma triglycerides among male and female strains, Related to Figure 1

(A) Mesenteric fat mass in male (black) and female (red) mice after 8 weeks of HF/HS feeding. Error bars represent SEM.

(B) Plasma triglyceride levels in male (black) and female (red) mice after 8 weeks of HF/HS feeding. Error bars represent SEM.

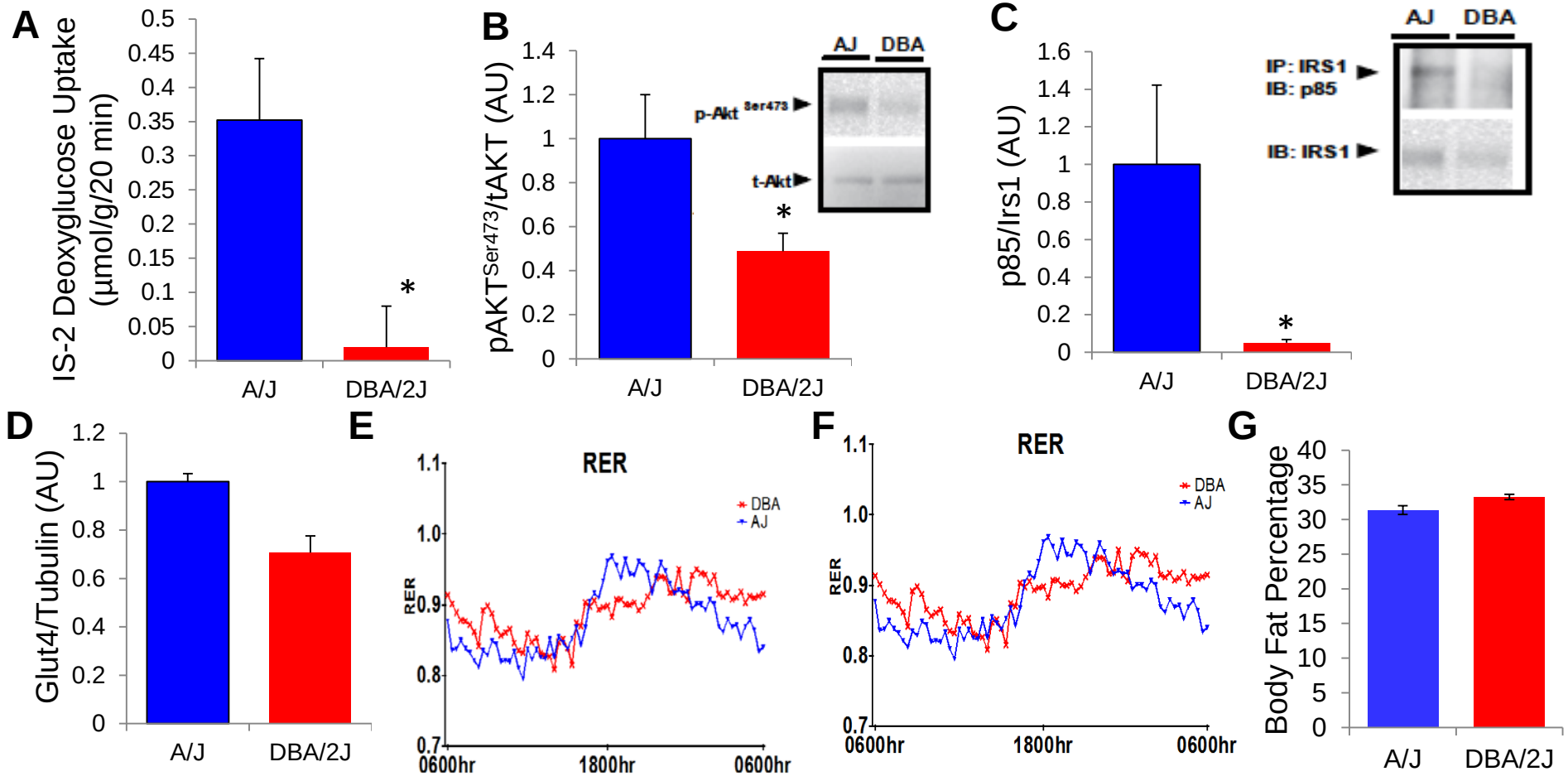

Figure S3. Molecular analysis of IR in A/J and DBA/2J strains of mice, Related to Figure 2

(A) Average uptake of deoxyglucose in isolated soleus muscle *in vitro* after insulin stimulation.

(B) Immunoblot analysis to detect phosphorylation of Akt on Serine 473, Average densitometry shown and representative immunoblot shown in inset.

(C) Insulin receptor substrate-1 (IRS)-1 activation was assesed by immunoprecipitation and immunoblot analysis of phosphatidylinositol (PI) 3-kinase p85 subunit association

(D) Average expression of Glut4 protein expression in soleus muscle of A/J and DBA/2J mice.

(E) Activity represented by number of beam breaks in A/J and DBA/2J mice after 8 weeks of HF/HS feeding during a 24 hour light/dark cycle.

(F) Respiratory exchange ratio (RER) in A/J and DBA/2J mice after 8 weeks of HF/HS feeding during a 24 hour light/dark cycle.

(G) Body fat percentage in A/J and DBA/2J mice after 8 weeks of HF/HS feeding.

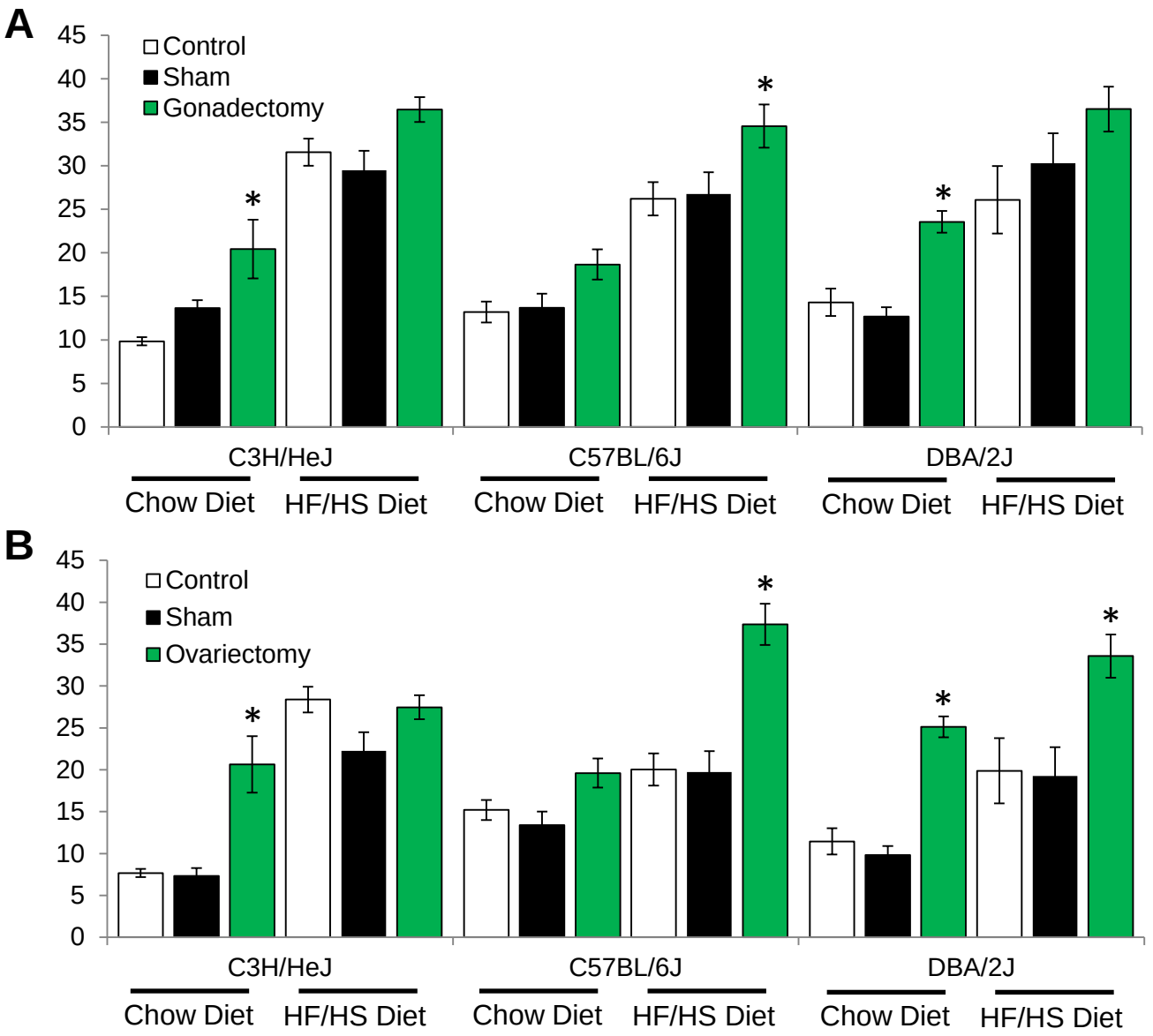

Figure S4. Body Fat Percentage in gonadectomized and ovariectomized mice, Related to Figure 2
(A) Average body fat percentage in male C3H/HeJ, C57BL/6J and DBA/2J mice after gonadectomy, Sham or control and being maintained on a chow or HF/HS diet for 8 weeks.
(B) Average body fat percentage in female C3H/HeJ, C57BL/6J and DBA/2J mice after ovariectomy, Sham or control and being maintained on a chow or HF/HS diet for 8 weeks. Asterisk (*) indicates significance of $p < 0.05$

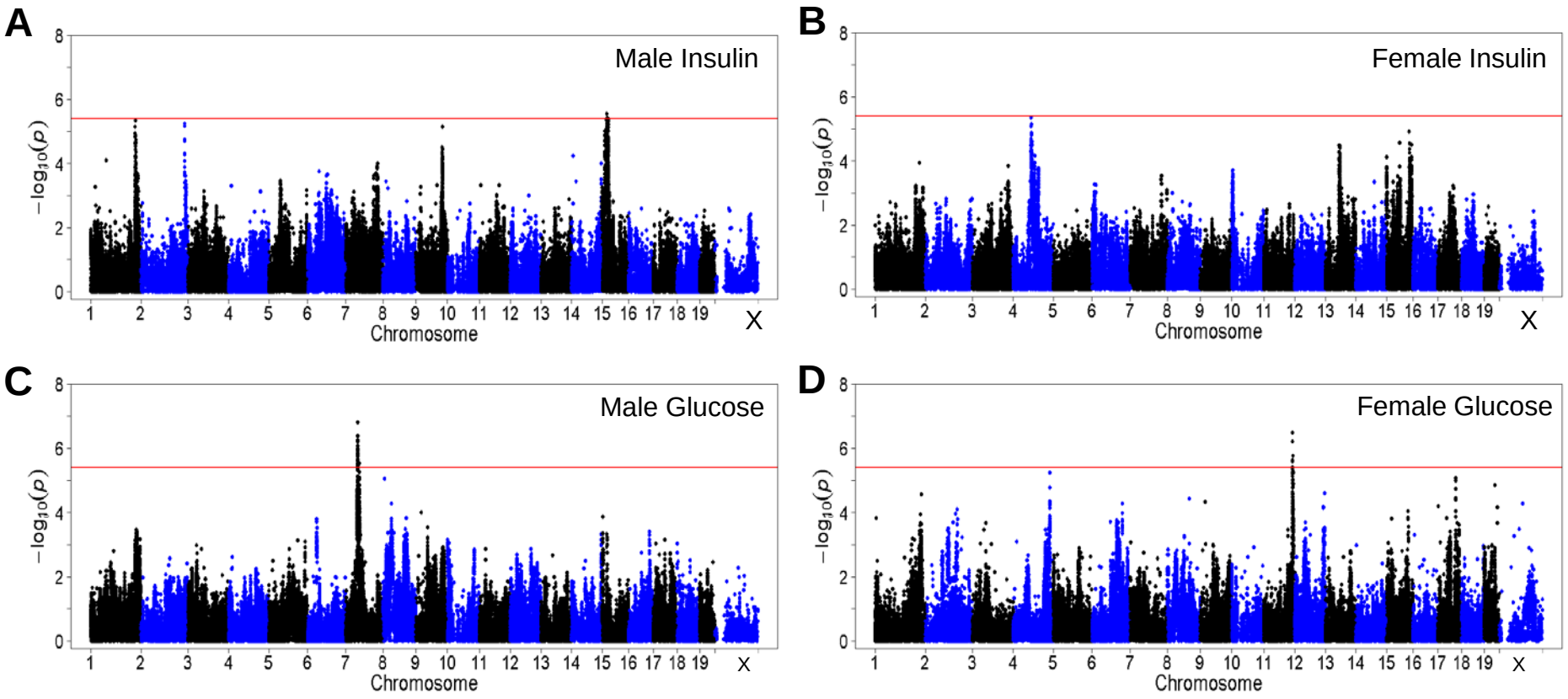

Figure S5. GWAS for plasma insulin and glucose levels in male and female mice, Related to Figure 3
(A-B) Manhattan plot showing the significance (–log10 of p) of all SNPs and plasma insulin levels after 8 weeks of HF/HS feeding in male mice (A) and female mice (B).
(C-D) Manhattan plot showing the significance (–log10 of p) of all SNPs and plasma glucose levels after 8 weeks of HF/HS feeding in male mice (C) and female mice (D).

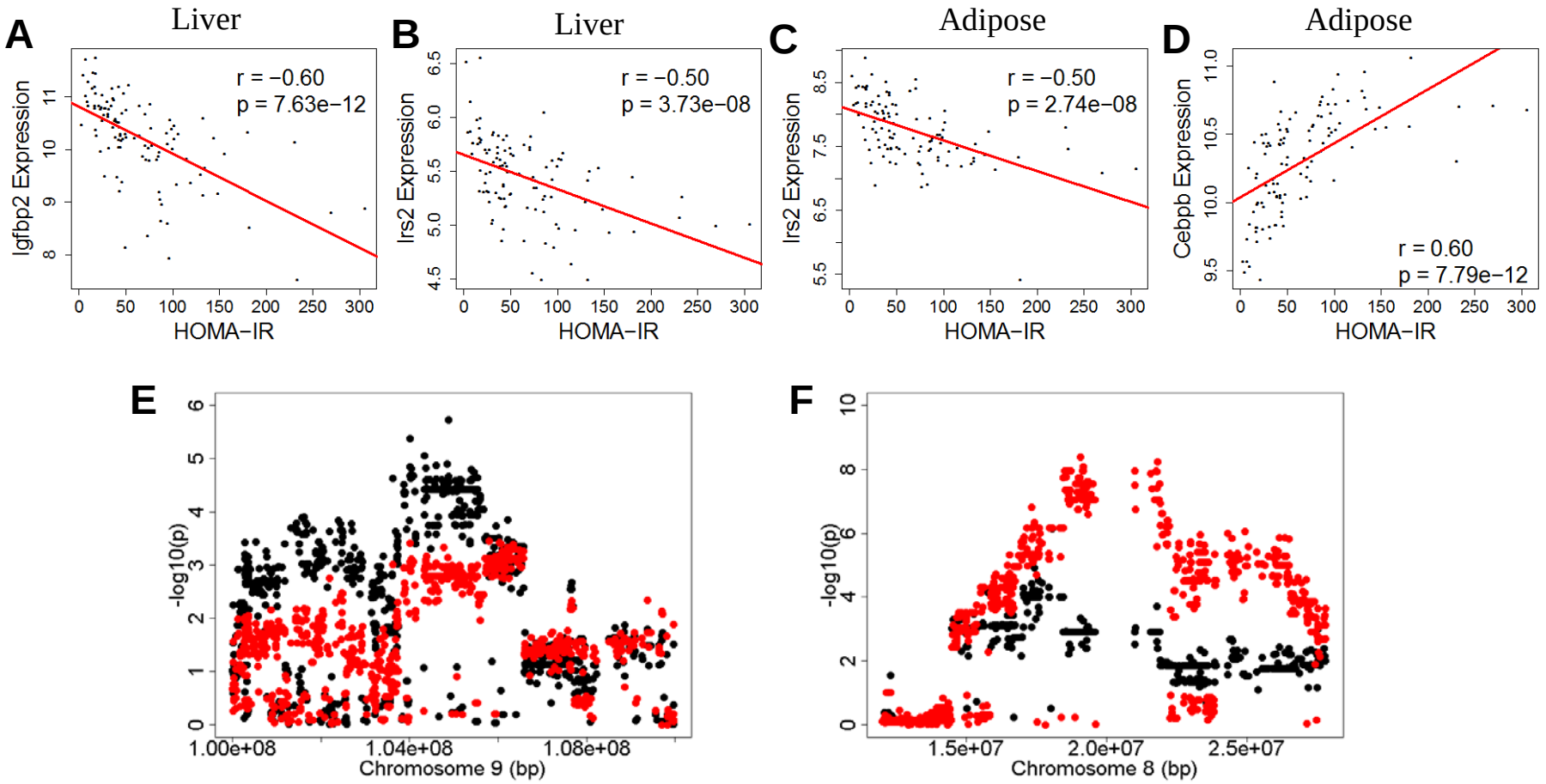

Figure S6. Correlation of gene expression in adipose and liver with HOMA-IR, Related to Figure 4.

(A) Correlation of Igfbp2 expression in liver tissue with HOMA-IR, regression line (red). r, biweight midcorrelation; p, p value.

(B) Correlation of Irs2 expression in liver tissue with HOMA-IR, regression line (red). r, biweight midcorrelation; p, p value.

(C) Correlation of Irs2 expression in gonadal adipose tissue with HOMA-IR, regression line (red). r, biweight midcorrelation; p, p value.

(D) Correlation of Cebpb expression in gonadal adipose tissue with HOMA-IR, regression line (red). r, biweight midcorrelation; p, p value.

(E) Locus plot for genome-wide significant association with HOMA-IR in male mice at chromosome 9 (Black dots) and eQTL for Acad11 (Red dots) in adipose tissue overlayed.

(F) Locus plot for genome-wide significant association with plasma insulin levels in male BXD RI mice at chromosome 8 (Black dots) and eQTL for Agpat5 (Red dots) in adipose tissue overlayed.

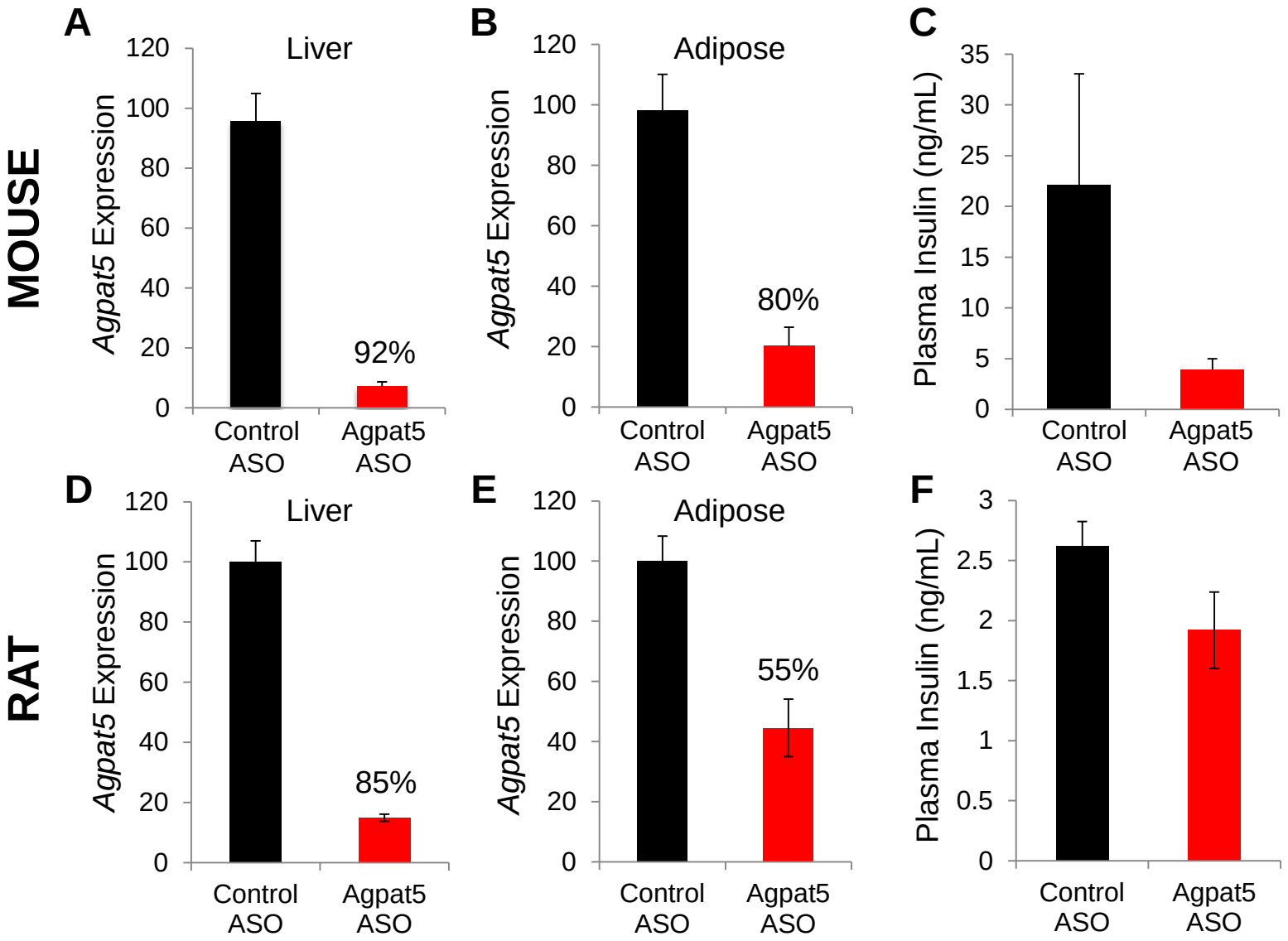

Figure S7. Antisense Oligonucleotide knockdown of liver and Adipose Agpat5 expression. Related to Figure 6

(A-B) Quantitative PCR analysis of *Agpat5* expression in liver (A) and adipose (B) tissue from mice treated with control ASO or Agpat5 ASO.

(C) Plasma insulin levels in mice treated with control ASO or Agpat5 ASO.

(D-E) Quantitative PCR analysis of *Agpat5* expression in liver (D) and adipose (E) tissue from rats treated with control ASO or Agpat5 ASO.

(F) Plasma insulin levels in rats treated with control ASO or Agpat5 ASO.

Table S1. Inbred and Recombinant Inbred Strains Included in Study, Related to Figure 1

Inbred Strains			Recombinant Inbred Strains					
Strain	Male	Female	Strain	Male	Female	Strain	Male	Female
129X1/SvJ	2	8	AXB10/PgnJ	3	4	BXD1/TyJ	3	3
A/J	6	11	AXB12/PgnJ	6	7	BXD11/TyJ		3
AKR/J	4	10	AXB13/PgnJ	3	7	BXD12/TyJ	6	6
BALB/cJ	12	16	AXB15/PgnJ	3	4	BXD13/TyJ	4	3
BTBR T<+> tf/J	7	8	AXB19/PgnJ	7	6	BXD14/TyJ	4	4
BUB/BnJ	8	11	AXB19a/PgnJ	5	7	BXD15/TyJ	2	8
C3H/HeJ	7	13	AXB19b/PgnJ	5	5	BXD16/TyJ		4
C57BL/6J	15	24	AXB2/PgnJ		3	BXD18/TyJ		3
C57BLKS/J	8	8	AXB4/PgnJ	4		BXD19/TyJ	4	8
C57L/J		7	AXB5/PgnJ	5	4	BXD21/TyJ	9	7
C58/J	2	7	AXB6/PgnJ	2	2	BXD24/TyJ	7	7
CBA/J	4	5	AXB8/PgnJ		8	BXD27/TyJ	7	
CE/J	10	10	BXA1/PgnJ	7	3	BXD31/TyJ	3	2
DBA/2J	14	21	BXA11/PgnJ	3	8	BXD32/TyJ	4	7
FVB/NJ	7	11	BXA12/PgnJ		4	BXD34/TyJ	4	8
I/LnJ	6	5	BXA13/PgnJ		3	BXD36/TyJ		4
KK/HlJ	5	7	BXA14/PgnJ	4	6	BXD38/TyJ	6	5
LG/J		8	BXA16/PgnJ	6	3	BXD39/TyJ		6
LP/J	4		BXA2/PgnJ	7	16	BXD40/TyJ	8	4
MA/MyJ	6	9	BXA24/PgnJ	6	10	BXD43/RwwJ	5	7
NOD/ShiLtJ	2	2	BXA4/PgnJ	4	7	BXD44/RwwJ	6	7
NON/ShiLtJ	6	6	BXA7/PgnJ	14	13	BXD45/RwwJ	5	6
NZB/BlNJ	4	8	BXA8/PgnJ	7	6	BXD48/RwwJ	9	8
NZW/LacJ	7	6	BXH19/TyJ	3	6	BXD49/RwwJ	4	4
PL/J	6	6	BXH2/TyJ		3	BXD5/TyJ	2	5
RIIIS/J	8	8	BXH20/KccJ	3	3	BXD50/RwwJ	6	5
SEA/GnJ	8	8	BXH22/KccJ	7	6	BXD51/RwwJ	4	4
SJL/J	6	8	BXH4/TyJ		4	BXD55/RwwJ	11	9
SM/J	6	5	BXH6/TyJ	8	7	BXD56/RwwJ	2	9
SWR/J	7	10	BXH8/TyJ	4	3	BXD6/TyJ	2	7
			BXH9/TyJ	3	7	BXD60/RwwJ	7	4
			CXB11/HiAJ	8	6	BXD61/RwwJ	8	7
			CXB12/HiAJ	8	7	BXD62/RwwJ	6	12
			CXB13/HiAJ	9	7	BXD64/RwwJ	8	7
			CXB3/ByJ	6	7	BXD66/RwwJ	7	7
			CXB4/ByJ	6	6	BXD68/RwwJ	7	6
			CXB6/ByJ	6	7	BXD69/RwwJ	2	
			CXB7/ByJ	7	7	BXD70/RwwJ	9	6
						BXD71/RwwJ	9	9
						BXD73/RwwJ	7	11
						BXD74/RwwJ	6	6
						BXD75/RwwJ	4	7
						BXD79/RwwJ	6	10
						BXD8/TyJ		2
						BXD84/RwwJ	12	10
						BXD85/RwwJ	6	8
						BXD86/RwwJ	7	8
						BXD87/RwwJ	8	8
						BXD9/TyJ	4	4

Table S2. Significant cis expression QTL and Metabolites at HOMA-IR, Related to Figure 4

Trait	Chr	Peak SNP	Tissue	Gene or Metabolite	Gene Start Position	pvalue
HOMA-IR	1	rs32316569	Adipose	Mndal	173857220	1.50E-39
			Adipose	Pyhin1	173630859	9.65E-29
			Adipose	Grem2	174833785	5.43E-11
			Adipose	Ifi203	173920407	5.36E-10
			Adipose	Fh1	175600374	0.000179
			Adipose	Cadm3	173334254	0.001
			Liver	Mndal	173857220	2.24E-47
			Liver	Fmn2	174501825	7.95E-17
			Liver	Ifi203	173920407	3.02E-12
			Plasma Metabolites	glycerol	NA	0.00234991
			Plasma Metabolites	taurine	NA	0.0095629
HOMA-IR	9	rs36804270	Adipose	Parp3	106470322	8.40E-22
			Adipose	Ppm1m	106194172	1.04E-18
			Adipose	Glyctk	106152857	1.33E-16
			Adipose	Dusp7	106368632	3.51E-14
			Adipose	Abhd14b	106448640	4.22E-13
			Adipose	Ackr4	104098138	1.68E-12
			Adipose	Abhd14a	106440051	3.86E-12
			Adipose	Pik3r4	105642995	2.62E-07
			Adipose	Nudt16	105129338	6.55E-06
			Adipose	Atp2c1	105403539	4.59E-05
			Adipose	Acy1	106432996	0.000228
			Adipose	Twf2	106203108	0.000246
			Adipose	Uba5	104046599	0.000272
			Adipose	Acad11	104040662	0.00033
			Liver	Abhd14b	106448640	2.74E-18
			Liver	Ppm1m	106194172	3.78E-17
			Liver	Abhd14a	106440051	4.04E-12
			Liver	Acy1	106432996	3.93E-08
			Liver	Mrpl3	105053239	8.75E-08
			Liver	Pcbp4	106453838	1.14E-07
			Liver	Glyctk	106152857	1.46E-07
			Liver	1300017J02Rik	103250522	2.10E-06
			Liver	Nudt16	105129338	2.68E-06
			Liver	Parp3	106470322	4.93E-05
			Liver	Uba5	104046599	0.000295
			Liver	Dusp7	106368632	0.000407
			Liver	Pcbp4	106453838	0.00041
			Liver	Pik3r4	105642995	0.000687
			Liver	Acpp	104288251	0.000792
			Plasma Metabolites	Arginine	NA	0.000676
			Plasma Metabolites	Niacinamide	NA	0.009976

Table S3. Top 50 Liver Genes Correlated With HOMA-IR, Related to Figure 4

Rank	r	p	Gene symbol
1	-0.65	2.05E-23	Igfbp2
2	-0.60	1.60E-19	Fbxo21
3	0.60	2.85E-19	Rcan1
4	0.58	1.21E-17	Mogat1
5	0.57	1.61E-17	Cd36
6	0.57	2.18E-17	Anxa2
7	-0.56	1.12E-16	Avpr1a
8	-0.56	2.41E-16	Apom
9	-0.55	6.05E-16	Abca8a
10	0.55	8.11E-16	Smarca4
11	0.54	1.35E-15	Uck1
12	0.54	1.67E-15	S100a10
13	0.54	1.94E-15	Ermp1
14	0.54	2.37E-15	Exoc4
15	0.54	4.36E-15	Tmem43
16	-0.53	6.30E-15	Rbbp4
17	0.53	7.53E-15	Dak
18	0.53	1.05E-14	Entpd5
19	0.53	1.38E-14	Spc25
20	-0.53	1.95E-14	Irs2
21	0.52	2.03E-14	Chpt1
22	0.52	2.37E-14	Hsd17b12
23	0.52	2.70E-14	Gpc1
24	0.52	6.04E-14	Ccng1
25	-0.51	7.79E-14	Foxp1
26	-0.51	1.26E-13	Cyp27a1
27	0.51	2.41E-13	Lgals1
28	0.50	3.52E-13	Fam73b
29	-0.50	3.63E-13	Scarb1
30	-0.50	3.72E-13	Pdia5
31	0.50	4.01E-13	Ptrh2
32	-0.50	6.18E-13	Fermt2
33	-0.50	6.23E-13	Gpld1
34	0.50	6.77E-13	Xpot
35	0.50	8.61E-13	Cmpk1
36	-0.49	9.39E-13	Srsf5
37	0.49	9.54E-13	Mad2l1
38	-0.49	1.01E-12	Maf1
39	0.49	1.35E-12	Wfdc2
40	0.48	3.99E-12	Fmo5
41	0.48	4.66E-12	Smc2
42	-0.48	4.68E-12	Slc8b1
43	-0.48	4.80E-12	Ces2a
44	0.48	5.08E-12	Ces2e
45	-0.48	5.16E-12	Fetub
46	0.48	5.19E-12	Mettl9
47	-0.48	6.68E-12	Rpl10a
48	0.48	6.77E-12	Srxn1
49	-0.48	9.45E-12	Cyp1a2
50	0.47	9.68E-12	BC029722

Table S4. Top 50 Adipose Genes Correlated With HOMA-IR, Related to Figure 4

Rank	r	p	Gene symbol
1	-0.64	5.87E-24	Chst1
2	-0.63	1.68E-23	Pde1a
3	-0.63	3.59E-23	Tab3
4	-0.62	9.36E-23	Rrm2b
5	-0.62	5.03E-22	Jup
6	-0.61	9.26E-22	Zrsr1
7	-0.61	1.09E-21	Xpc
8	-0.61	1.87E-21	Chrdl1
9	-0.61	2.54E-21	Sort1
10	-0.60	5.45E-21	Ndrg1
11	-0.60	5.84E-21	Cfd
12	0.60	7.68E-21	Cd72
13	-0.60	1.25E-20	Ube2h
14	-0.60	1.26E-20	Ganc
15	-0.60	1.67E-20	Agbl3
16	-0.60	1.70E-20	Pink1
17	-0.59	2.63E-20	Cenpv
18	-0.59	3.78E-20	Ivns1abp
19	0.59	3.81E-20	Cebpb
20	-0.59	3.82E-20	2310010J17Rik
21	-0.59	4.09E-20	Pck1
22	0.59	4.71E-20	Dnmt3l
23	-0.59	4.91E-20	Mgst3
24	-0.59	5.80E-20	Gm10374
25	-0.59	5.96E-20	Apcdd1
26	-0.59	6.07E-20	Osbpl1a
27	0.59	6.33E-20	Dhcr7
28	-0.59	6.81E-20	Nrbp2
29	0.59	8.11E-20	Dera
30	0.59	1.06E-19	Spc25
31	0.58	2.99E-19	Csk
32	-0.58	4.05E-19	Gkap1
33	-0.58	4.50E-19	Tmem134
34	-0.58	4.99E-19	Hoxa7
35	-0.58	5.79E-19	Anapc13
36	0.58	7.60E-19	Asf1b
37	-0.57	8.36E-19	Ophn1
38	-0.57	8.60E-19	Glrx2
39	0.57	1.06E-18	Mvd
40	-0.57	1.28E-18	Adh5
41	-0.57	1.62E-18	Surf1
42	-0.57	1.62E-18	Ncor1
43	-0.57	1.92E-18	Fdx1
44	-0.57	1.96E-18	Irs2
45	0.57	3.17E-18	Nedd4l
46	-0.57	3.38E-18	Ghr
47	-0.57	3.75E-18	Mst1r
48	0.57	3.97E-18	Plin2
49	-0.57	4.20E-18	Las1l
50			

Table S5. Genome-wide significant plasma metabolite QTL (mQTL), Related to Figure 5

Trait	Chr.	Peak SNP	Position (Mb)	P-Value	MAF	LD	No. of Genes
Adenosine	13	rs6399032	5387909	1.07E-07	0.055	3.0-12.2	35
Adenosine	6	rs50509130	12586105	1.08E-07	0.054	12.5-15.8	11
Adenosine	17	rs50773521	49379896	3.10E-06	0.057	48.1-49.4	17
Adenosine	19	rs37149042	24778607	3.57E-06	0.054	24.2-25.2	9
Adenosine	11	rs26906284	68380725	3.60E-06	0.054	67.8-68.4	5
Adenosine	17	rs49862571	72179790	3.33E-06	0.059	71.1-72.3	17
Cystamine	7	rs50538240	148061082	3.09E-08	0.20	147.4-149.4	77
Glutamine	6	rs37155646	31876349	2.35E-06	0.081	27.7-32.0	40
Glycerol	3	rs31076351	62716836	1.95E-07	0.086	60.9-65.2	19
Glycerol	14	rs51980658	101088554	5.46E-07	0.054	100.0-113.0	24
Glycerol	15	rs31600615	79165941	9.66E-07	0.12	79.1-79.2	3
Glycerol	8	rs32824270	47366716	9.68E-07	0.087	44.5-48.1	28
Glycerol	8	rs51588257	12302705	1.21E-06	0.054	8.8-12.7	25
Glycerol	19	rs30767320	19916451	1.95E-06	0.40	17.0-20.1	9
Glycerol	16	rs33359909	75508760	2.33E-06	0.06	75.5-77.2	6
Glycerol	15	rs31901221	18654064	3.86E-06	0.054	16.4-20.7	3
Kynurenic Acid	11	rs3661285	90007992	2.62E-06	0.075	87.1-93.0	43
Phosphocholine	2	rs27441517	119932775	5.04E-08	0.065	119.4-120.0	15
2 Deoxyadenosine	12	rs37817859	107067975	2.88E-06	0.13	106.7-108.7	8
2 Deoxycytidine	12	rs46185976	4372561	6.43E-07	0.092	3.7-4.4	9
2 Deoxycytidine	1	rs31934447	11125015	1.85E-06	0.12	9.5-12.9	15
5 Adenosylhomocysteine	9	rs51650764	108758191	3.49E-06	0.18	107.5-108.8	44
Xanthosine	9	rs30133859	86031934	8.09E-07	0.49	85.3-88.0	12

Supplemental Experimental Procedures

Hyperinsulinemic-euglycemic clamp studies. At 20 weeks of age, dual catheters were surgically placed in the right jugular vein and glucose clamp studies were performed 3 days post-surgery as previously described (Hevener et al., 2003; Hevener et al., 2007; Ribas et al., 2011). Briefly, all animals were fasted for 6 hours prior to the clamp and studied in the conscious state. Basal glucose turnover was determined following a 90-minute constant infusion of (5.0 μCi/h, 0.12 ml/h) of [3-^{3}H] D-glucose (Perkin Elmer). After the basal period, glucose (50% dextrose, Abbott Laboratories) and insulin (8 mU/kg/min, Novo Nordisk Pharmaceutical Industries) plus tracer (5.0 μCi/h) infusions were initiated simultaneously, and glucose levels clamped at euglycemia using a variable glucose infusion rate (GIR). At steady state the total glucose disposal rate (GDR), measured by tracer dilution technique, is equal to the sum of the rate of endogenous or hepatic glucose production (HGP) and the exogenous (cold) glucose infusion rate (GIR)(Hevener et al., 2003; Hevener et al., 2007; Steele, 1959). The insulin-stimulated component of the total GDR (IS-GDR) is equal to the total GDR minus the basal glucose turnover rate.

***Ex-vivo* soleus muscle strip glucose uptake.** Whole muscle ex-vivo glucose uptake was assessed using 2-deoxyglucose, with minor changes to that described previously (McCurdy and Cartee, 2005; Ribas et al., 2011). Briefly, soleus muscles were carefully excised from anaesthetized animals and immediately incubated for 30 minutes at 35ºC in complete Krebs-Henseleit buffer with or without 60μU/ml insulin. Muscles were then transferred to the same buffer containing 3mCi/ml ^{3}H-2-deoxy-glucose and 0.053mCi/ml 14C-mannitol, and incubated for exactly 20 minutes prior to snap freezing. Muscles were homogenized in lysis buffer and counted for radioactivity or subjected to western blotting. Glucose uptake was standardized to the non-specific uptake of mannitol and expressed as μmol of glucose uptake per gram of tissue.

Association Analysis. Genotypes for all strains of mice (**Table S1**) were obtained from Jackson Laboratories using the Mouse Diversity Array (Yang et al., 2009). After removing SNPs that were flagged as poor quality, 459,911 SNPs remained. Genome-wide association of clinical traits, adipose and liver expression data was performed using FaST-LMM which uses a linear mixed model to correct for population structure (Lippert et al., 2011). Our analyses indicate this

method can appropriately account for the population structure; however, it is possible that small segments of relatedness on certain chromosomes might be confounding. The SNPs used were filtered to have a minor allele frequency of >5% and missing genotype rate <10%. To avoid proximal contamination and still achieve a reasonable run-time, the following procedure was used: when testing the SNPs on each chromosome N for association, the relatedness matrix used to correct for population structure was generated from all the SNPs not on chromosome N. Significance threshold of (3.46×10^{-6}) was determined through permutation and modeling (Bennett et al., 2010). Linkage disequilibrium (LD) was determined by calculated pairwise r^2 SNP correlations for each chromosome. LD boundaries were determined by visualizing $r^2 > 0.8$ correlations in MATLAB (MathWorks).

Supplemental References

Bennett, B.J., Farber, C.R., Orozco, L., Kang, H.M., Ghazalpour, A., Siemers, N., Neubauer, M., Neuhaus, I., Yordanova, R., Guan, B., *et al.* (2010). A high-resolution association mapping panel for the dissection of complex traits in mice. Genome Res *20*, 281-290.

Hevener, A.L., He, W., Barak, Y., Le, J., Bandyopadhyay, G., Olson, P., Wilkes, J., Evans, R.M., and Olefsky, J. (2003). Muscle-specific Pparg deletion causes insulin resistance. Nat Med *9*, 1491-1497.

Hevener, A.L., Olefsky, J.M., Reichart, D., Nguyen, M.T., Bandyopadyhay, G., Leung, H.Y., Watt, M.J., Benner, C., Febbraio, M.A., Nguyen, A.K., *et al.* (2007). Macrophage PPAR gamma is required for normal skeletal muscle and hepatic insulin sensitivity and full antidiabetic effects of thiazolidinediones. J Clin Invest *117*, 1658-1669.

Lippert, C., Listgarten, J., Liu, Y., Kadie, C.M., Davidson, R.I., and Heckerman, D. (2011). FaST linear mixed models for genome-wide association studies. Nat Methods *8*, 833-835.

McCurdy, C.E., and Cartee, G.D. (2005). Akt2 is essential for the full effect of calorie restriction on insulin-stimulated glucose uptake in skeletal muscle. Diabetes *54*, 1349-1356.

Ribas, V., Drew, B.G., Le, J.A., Soleymani, T., Daraei, P., Sitz, D., Mohammad, L., Henstridge, D.C., Febbraio, M.A., Hewitt, S.C., *et al.* (2011). Myeloid-specific estrogen receptor alpha deficiency impairs metabolic homeostasis and accelerates atherosclerotic lesion development. Proc Natl Acad Sci U S A *108*, 16457-16462.

Steele, R. (1959). Use of C14-glucose to measure hepatic glucose production following an intravenous glucose load or after injection of insulin. Metabolism *8*, 512-519.

Yang, H., Ding, Y., Hutchins, L.N., Szatkiewicz, J., Bell, T.A., Paigen, B.J., Graber, J.H., de Villena, F.P., and Churchill, G.A. (2009). A customized and versatile high-density genotyping array for the mouse. Nat Methods *6*, 663-666.